Structure of the Maule earthquake rupture zone: insights from seismic tomography

Stephen P. Hicks[1], Andreas Rietbrock[1], Isabelle M.A. Ryder[1], Matthew Miller[2], Chao-Shing Lee[3], Christian Haberland[4], Mark Simons[5] & Andrés Tassara[2]

[1] School of Environmental Sciences, University of Liverpool, U.K., [2] Departmento de Geofisica, Universidad de Concepción, Concepción, Chile [3], Institute of Applied Geosciences, National Taiwan Ocean University, Taiwan, [4] GFZ German Research Centre of Geosciences, Potsdam, Germany, [5] Seismological Laboratory, Geological and Planetary Sciences, Caltech, Pasadena, United States

Email: ***s.hicks@liverpool.ac.uk*** Web: ***http://pcwww.liv.ac.uk/~es0u719b***

MAULE EARTHQUAKE WORKSHOP
March 4-8 2013
Concepción, Chile

1. Introduction

The 2010 Maule, Chile earthquake is currently the 6th largest earthquake to have been recorded. It provides an opportunity to investigate the factors governing energy release and deformation along subduction megathrusts.

Published co-seismic slip distribution (e.g. Moreno et al., 2012) and aftershock distributions (e.g. Rietbrock et al., 2012) imply rupture zone properties vary spatially.

Such variations can be viewed within the subduction zone asperity/barrier framework. Heterogeneity within the rupture zone may be expressed in seismic properties.

We image the seismic velocity structure of the Maule region by using travel-time data from aftershocks. Data primarily come from the International Maule Aftershock Deployment (IMAD). Most aftershock seismicity and co-seismic slip is concentrated seaward of the Chilean coastline.

Using the onshore recordings alone inherently fails to resolve the offshore aftershock locations and offshore velocity structure well (Section 3). We have incorporated data from offshore ocean-bottom seismometer (OBS) networks to improve our understanding of the offshore region (Section 4).

2. Inversion method

- Use VELEST to invert for 1D P- & S-wave velocity models, including station correction terms.
- Tomographic inversion using SIMUL2000 (Thurber, 1983) - weighted least squares approach.
- Direct determination of Vp / Vs ratio by inverting for S-P travel times
- Staggered inversion scheme (e.g. Haberland et al., 2009) to ensure that any potential artefacts are not propagated through to final model. See Hicks et al. (2012) for details.

3. First-order velocity structure

a) Inversion details

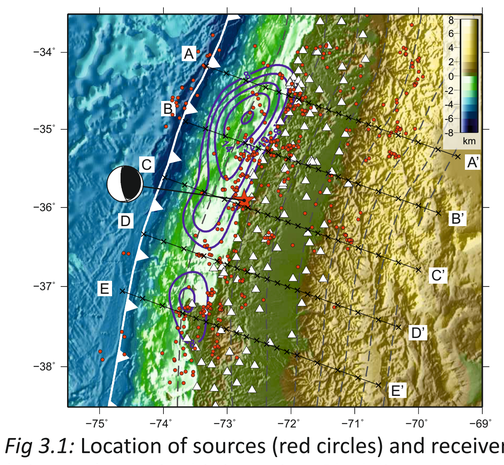

Fig 3.1: Location of sources (red circles) and receivers (triangles) used in this inversion. Black lines show the location of the slices through the 3D model.

Stations used: IMAD land stations only
Event catalogue: 397 events from March '10 to May '10
Travel-time picking method: automatic (STA/LTA algorithm
Number of picks: 48,000 (30,000 P & 19,000 S)
Initial locations: Relocated in 2D model for south-central Chile (Rietbrock et al., 2012)

b) 2D Velocity model

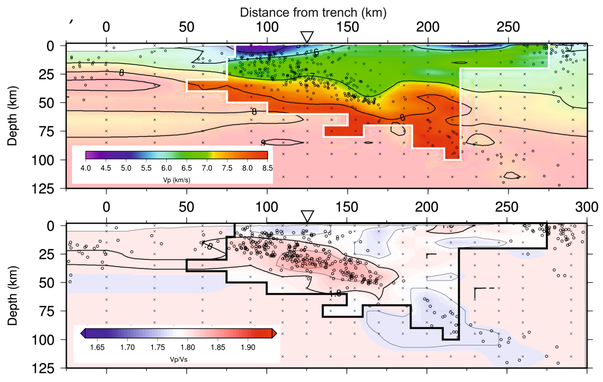

Fig. 3.2: Vp and Vp / Vs 2D velocity model sections

c) 3D Velocity model

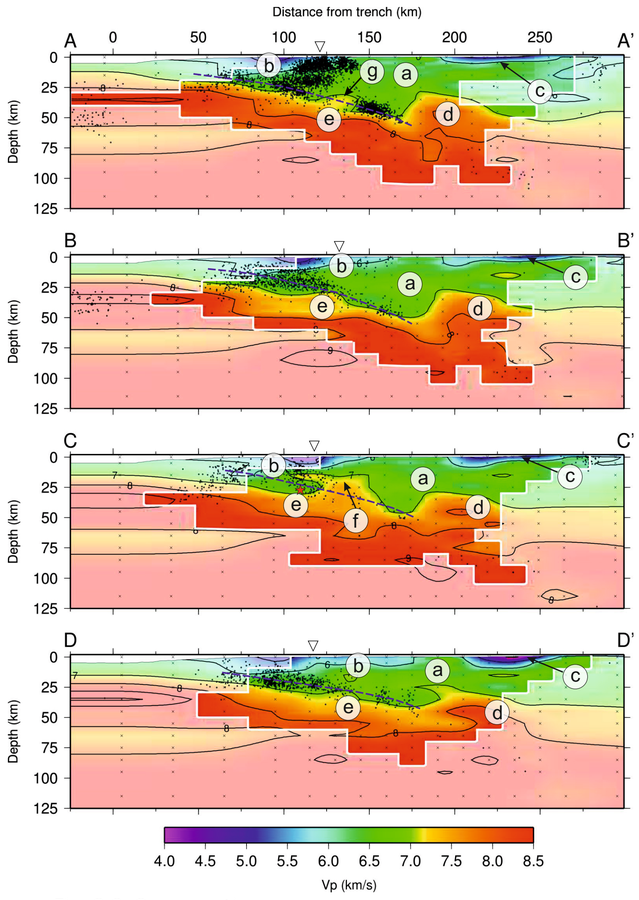

Fig. 3.3: Cross-sections through 3D P-wave velocity model

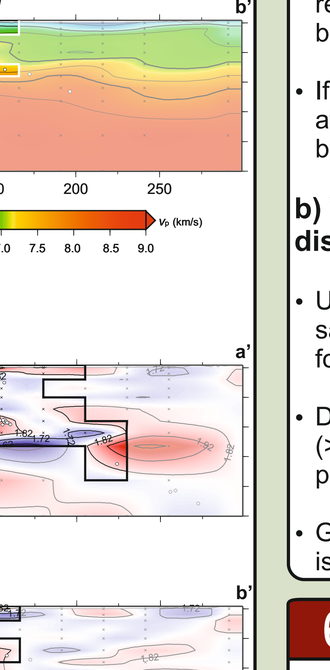

Fig. 3.4: Vp along plate interface and co-seismic slip model of Moreno et al. (2012)

d) Interpretation

***(a)* Continental crust**
Max. thickness 50 km beneath E. coastal ranges

***(b)* Marine forearc**

***(c)* Central depression basin**

***(d)* Continental mantle**
Intersection of continental Moho with interface coincides with maximum depth extent of seismogenic zone

***(e)* Subducting oceanic crust**
Interface dip angle ~12-18° correlates with prior estimates of regional slab geometry

***(f)* & *(g)* High Vp (and elevated Vp / Vs) anomalies**
One in mainshock nucleation area, and one beneath the Pichilemu region; both lie beneath coastline on top of the megathrust. Both protrude above interface by 4-10 km.

e) Comparison with forearc Bouguer gravity field

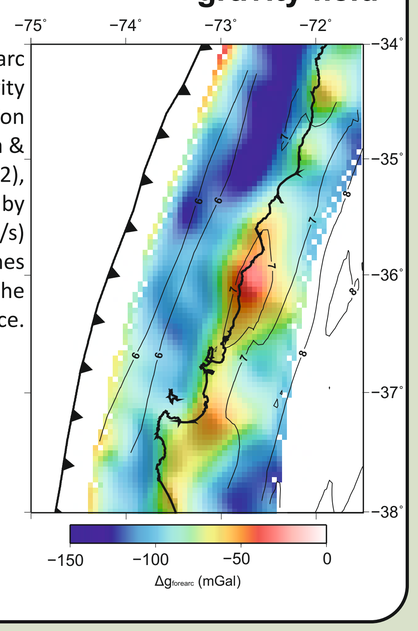

Fig. 3.5: Forearc Bouguer gravity contribution (Tassara & Echaurren, 2012), overlain by interface Vp (km/s) contour lines projected to the surface.

4. Shedding more light on the marine forearc

a) Inversion details & 1D locations

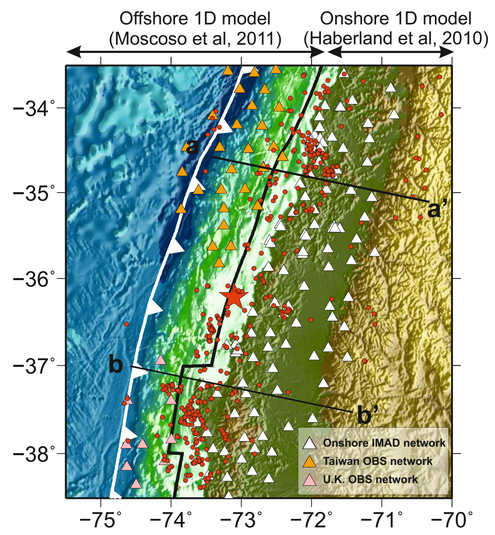

Fig. 4.1: Location of sources and receivers used in this inversion. Black line demarcates velocity models used to form 1D locations.

Stations used: IMAD land stations + Taiwanese OBS deployment (29 stations, Jul - Sept '10) + U.K. OBS deployment (9 stations, Aug '10 - Jan '11).
Event catalogue: 422 events from Mar '10 to Sept '10.
Travel-time picking method: Hand-picked.
Number of picks: 37,000 (26,000 P & 11,000 S)
Initial locations: Two separate 1D velocity models: onshore and offshore depending on epicentral location (see *Fig 4.1*).

b) 2D Velocity model

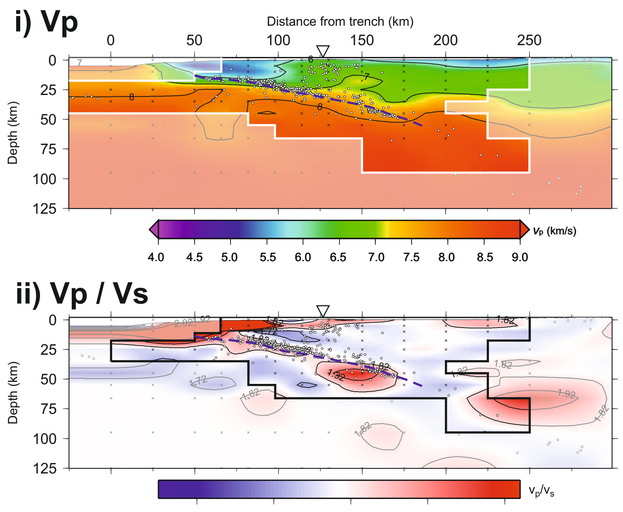

Fig 4.2: 2D velocity models with estimated thrust interface geometry (dashed line).

c) Relationship between velocity structure, seismicity & slip

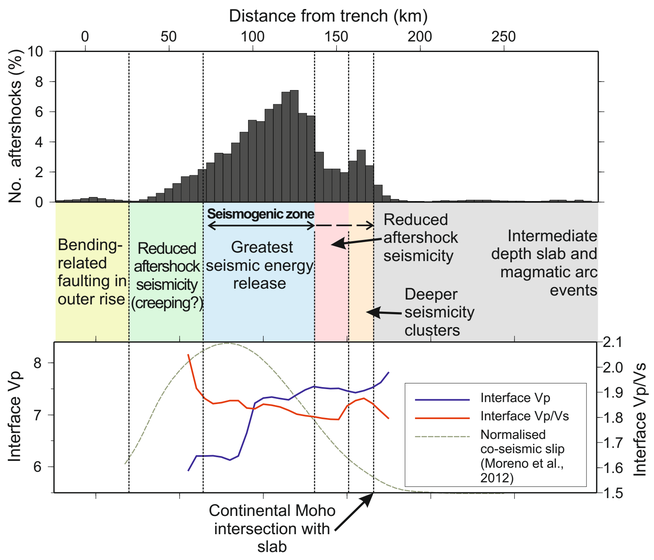

Fig 4.3: Histogram of events from catalogue of Rietbrock et al. (2012) and seismic velocity structure along thrust interface.

d) 3D Velocity model

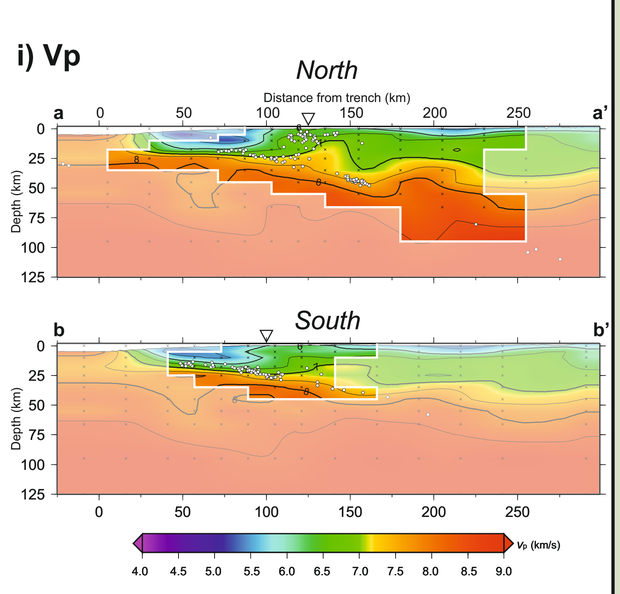

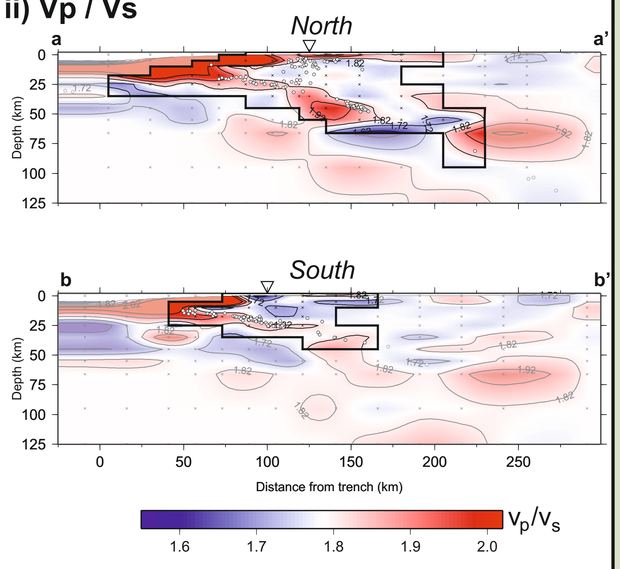

Fig 4.4: 3D Vp and Vp/Vs models. Both sections are oriented perpendicular to the trench and cross through the Pichilemu and Arauco areas of the rupture zone, respectively (Locations on *Fig. 4.1*).

5. Summary

a)Velocity/gravity anomaly in Darwin Gap

- Velocity anomaly is compositionally similar to hydrated oceanic crust or mantle.
- Anomaly does not correlate with surface outcrops Paleozoic/Triassic granitoids.
- Cannot reconcile with tomography alone whether seamount structure is attached to subducting crust.
- Down-dip of mainshock nucleation area, yet in a region of somewhat low co-seismic slip. How can it be classified within an asperity/barrier model?
- If sheared off, then aseismic creep may be occurring at its base. If it remains fully coupled, then it may still be locked, acting as a geometrical irregularity.

b) Velocity structure vs. seismicity distribution

- Up-dip seismogenic zone limit dominated by fluid-saturated sediments / oceanic crust in marine forearc (vp < 6.0 km/s, vp/vs > 2.00).
- Deep cluster of seismicity associated with high vp/vs (> 1.85). Located up-dip of continental moho. High pore fluid pressure & possible dehydration in slab?
- Greatest co-seismic slip occurred where megathrust is overlain by slower P-wave velocities.

6. References & acknowledgements

Haberland, C., A. Rietbrock, D. Lange, K Bataille, and T. Dahm (2009), Structure of the seismogenic zone of the southcentral Chilean margin revealed by local earthquake travel-time tomography, J. Geophys. Res.., 114, B01317.

Hicks, S.P., et al (2012), The 2010 Mw8.8 Maule, Chile earthquake: Nucleation and rupture propagation controlled by subducted topographic high, Geophys. Res. Lett.., 39, L19308.

Moreno, M., et al. (2012), Toward understanding tectonic control on the Mw 8.8 2010 Maule, Chile earthquake, Earth Planet. Sci. Lett., 321-322, 152-165.

Moscoso, E., et al. (2011), Revealing the deep structure and rupture plane of the 2010 Maule, Chile earthquake (Mw=8.8) using wide angle seismic data, Earth Planet. Sci. Lett, 307, 147-155.

Rietbrock, A., et al. (2012), Aftershock seismicity of the 2010 Maule Mw = 8.8 Chile earthquake: Correlation between co-seismic slip models and aftershock distribution? Geophys. Res. Lett., 39, L08310.

Tassara, A. and A. Echaurren (2012), Anatomy of the Andean subduction zone: 3D density model upgraded and compared against global-scale models, Geophys. J. Int., 189, 161-168.

Thurber, C.H. (1983), Earthquake locatios and three-dimensional crustal structure in the Coyote Lake area, Central California, J. Geophys. Res., 88, 8226-8236.

We would like to thank all institutions and field crews that were involved with the deployment of seismic instruments in Chile. We also thank the local Chilean landowners for their continued support during the whole deployment time. S.P.H. is support by a NERC studentship.